

000  
001  
002  
003  
004  
005  
006  
007  
008  
009  
010  
011  
012  
013  
014  
015  
016  
017  
018  
019  
020  
021  
022  
023  
024  
025  
026  
027  
028  
029  
030  
031  
032  
033  
034  
035  
036  
037  
038  
039  
040  
041  
042  
043  
044  
045  
046  
047  
048  
049  
050  
051  
052  
053

THE COOPER UNION  
ALBERT NERKEN SCHOOL OF ENGINEERING

A Deep Partitioned Autoencoder  
for De-Noising Live Audio

by  
Ethan Lusterman

A thesis submitted in partial fulfillment  
of the requirements for the degree of  
Master of Engineering

September 2016

Professor Sam Keene, Advisor

054 THE COOPER UNION FOR THE  
055  
056 ADVANCEMENT OF SCIENCE AND ART  
057  
058  
059  
060

061 ALBERT NERKEN SCHOOL OF ENGINEERING  
062  
063  
064  
065  
066  
067  
068  
069

070 This thesis was prepared under the direction of the Can-  
071 didate's Thesis Advisor and has received approval. It was  
072 submitted to the Dean of the School of Engineering and  
073 the full Faculty, and was approved as partial fulfillment of  
074 the requirements for the degree of Master of Engineering.  
075  
076  
077  
078  
079  
080  
081  
082  
083  
084  
085  
086

087 \_\_\_\_\_  
088 Dean, School of Engineering                      Date  
089  
090  
091  
092  
093  
094

095 \_\_\_\_\_  
096 Prof. Sam Keene, Thesis Advisor                      Date  
097  
098  
099  
100  
101  
102  
103  
104  
105  
106  
107

108  
109  
110  
111  
112  
113  
114  
115  
116  
117  
118  
119  
120  
121  
122  
123  
124  
125  
126  
127  
128  
129  
130  
131  
132  
133  
134  
135  
136  
137  
138  
139  
140  
141  
142  
143  
144  
145  
146  
147  
148  
149  
150  
151  
152  
153  
154  
155  
156  
157  
158  
159  
160  
161

# Acknowledgements

Ack example

162  
163  
164  
165  
166  
167  
168  
169  
170  
171  
172  
173  
174  
175  
176  
177  
178  
179  
180  
181  
182  
183  
184  
185  
186  
187  
188  
189  
190  
191  
192  
193  
194  
195  
196  
197  
198  
199  
200  
201  
202  
203  
204  
205  
206  
207  
208  
209  
210  
211  
212  
213  
214  
215

# Abstract

## Abstract

216  
217  
218  
219  
220  
221  
222  
223  
224  
225  
226  
227  
228  
229  
230  
231  
232  
233  
234  
235  
236  
237  
238  
239  
240  
241  
242  
243  
244  
245  
246  
247  
248  
249  
250  
251  
252  
253  
254  
255  
256  
257  
258  
259  
260  
261  
262  
263  
264  
265  
266  
267  
268  
269

# Contents

<b>1</b>	<b>Introduction</b>	<b>1</b>
<b>2</b>	<b>Background</b>	<b>2</b>
2.1	Machine Learning . . . . .	2
2.1.1	Regression . . . . .	3
2.1.2	Overfitting and Curse of Dimensionality . . . . .	3
2.1.3	Loss functions and Regularization . . . . .	3
2.1.4	Gradient Stuff? . . . . .	3
2.2	Neural Networks . . . . .	3
2.2.1	Dense Layer . . . . .	3
2.2.2	Convolutional Layer . . . . .	3
2.2.3	Nonlinearity Choice . . . . .	3
2.3	Signals and Systems . . . . .	3
2.3.1	Signals . . . . .	3
2.3.2	Convolution . . . . .	4
2.3.3	Frequency Transforms . . . . .	5
2.3.4	Windowing and Perfect Reconstruction . . . . .	6
2.3.5	Window Size and Frequency v. Time Resolution Tradeoff	7
2.3.6	Noise and Signal-to-Noise Ratio . . . . .	7
2.3.7	Magnitude and Phase Spectrum . . . . .	7
<b>3</b>	<b>Signal Model and Data</b>	<b>8</b>
3.1	Network Input and Output . . . . .	8
3.2	Signal and Noise Choices . . . . .	9
3.3	Other Network Parameters . . . . .	10
<b>4</b>	<b>De-noising Architectures</b>	<b>11</b>
4.1	Classic Supervised Autoencoder . . . . .	11
4.2	Paris Autoencoder . . . . .	11
4.3	Partitioned Autoencoder . . . . .	11

270	4.3.1 Phase Reconstruction . . . . .	11
271		
272	4.4 Curro Autoencoder . . . . .	11
273		
274		
275	<b>5 Results</b>	<b>12</b>
276	5.1 Classic Supervised Autoencoder . . . . .	12
277		
278	5.2 Paris Autoencoder . . . . .	12
279		
280	5.3 Partitioned Autoencoder . . . . .	12
281		
282	5.4 Curro Autoencoder . . . . .	12
283		
284	<b>6 Conclusions and Future Work</b>	<b>13</b>
285		
286	6.1 Conclusions . . . . .	13
287		
288	6.2 Future Work . . . . .	13
289	6.2.1 Models . . . . .	13
290		
291	6.2.2 Data . . . . .	13
292		
293		
294		
295		
296		
297		
298		
299		
300		
301		
302		
303		
304		
305		
306		
307		
308		
309		
310		
311		
312		
313		
314		
315		
316		
317		
318		
319		
320		
321		
322		
323		

324  
325  
326  
327  
328  
329  
330  
331  
332  
333  
334  
335  
336  
337  
338  
339  
340  
341  
342  
343  
344  
345  
346  
347  
348  
349  
350  
351  
352  
353  
354  
355  
356  
357  
358  
359  
360  
361  
362  
363  
364  
365  
366  
367  
368  
369  
370  
371  
372  
373  
374  
375  
376  
377

## List of Figures

1	.....	12
---	-------	----

378	Table of Nomenclature
379	
380	
381	
382	
383	
384	
385	
386	
387	
388	
389	
390	
391	
392	
393	
394	
395	
396	
397	
398	
399	
400	
401	
402	
403	
404	
405	
406	
407	
408	
409	
410	
411	
412	
413	
414	
415	
416	
417	
418	
419	
420	
421	
422	
423	
424	
425	
426	
427	
428	
429	
430	
431	



# 1 Introduction

Advances in smartphone technology have led to smaller devices with more powerful audio hardware, allowing for common consumers to make higher quality recordings. However, recorded speech and music are subject to noisy conditions, often hampering intelligibility and listenability. The goal of denoising audio recordings is to improve intelligibility and perceived quality. A variety of applications of audio denoising exist, including listening to a recording of a band or an artist’s live performance in a noisy crowd, or listening to a recorded conversation or speech under noisy conditions.

A common technique for denoising involves the use of deep neural networks (DNN). [PARIS] Advances in parallel graphics processing units (GPU) and in machine learning algorithms have allowed for training deeper networks faster, utilizing more hidden layers with more neurons.

Prior work in denoising audio has involved access to noise-free training data. Since common consumers do not often have access to clean audio, we seek to denoise without the use of clean audio.

In this thesis, we compare several neural network architectures and problem scenarios, ranging from data input types, level of noise, depth of network, training objectives, and more. In Chapter 2, we present background information on machine learning, neural networks, and signal processing as well as prior work in audio denoising. In Chapter 3, we detail all considered network architectures. In Chapter 4, we compare results from different data inputs, levels of noise, network architectures, and training objectives and discuss methods of evaluation. Finally, we make conclusions and recommendations for future work in Chapter 5.

## 2 Background

### 2.1 Machine Learning

Machine learning involves the use of computer algorithms to make decisions based on training data. Generally, this falls into categorizing input data (classification) or determining a mathematical function to determine a continuous output given an input (regression). Popular classification examples include recognizing handwritten digits (MNIST) as well as determining whether an image contains a cat or a dog. (REF) An example of a regression problem is determining the temperature given a set of input features (humidity, latitude, longitude, date, etc.).

Problems where training data contain input data vectors as well as the correct output vectors (targets) are known as supervised learning problems. Training a model to denoise audio where noise was introduced to the clean audio would be a supervised learning problem. On the other hand, training a model to denoise audio where the underlying clean signal is not known is an unsupervised learning problem. Different loss functions and neural network architectures can be exploited to accomplish denoising without the clean data.

For the purposes of this thesis, we use machine learning to determine an underlying nonlinear function that removes noise from time slices of audio (i.e. regression). These slices can then be pieced back together through overlap-add resynthesis. To clarify, this is a general linear model that maps an input noisy audio vector  $y[n] = x[n] + N[n]$  to  $\tilde{x}[n]$ , a target denoised audio vector, where  $x[n]$  is the underlying clean signal and  $N[n]$  is the additive background noise.

### 2.1.1 Regression

A classical regression technique is linear regression, where one or more independent variables  $x_i$  are used to determine a scalar dependent variable  $y$ . The case of a single independent variable  $x$  is known as simple linear regression. On the other hand, the case of estimating A canonical example would be estimating a sine wave  $x[n]$  given noisy samples

### 2.1.2 Overfitting and Curse of Dimensionality

### 2.1.3 Loss functions and Regularization

### 2.1.4 Gradient Stuff?

## 2.2 Neural Networks

### 2.2.1 Dense Layer

### 2.2.2 Convolutional Layer

### 2.2.3 Nonlinearity Choice

## 2.3 Signals and Systems

Domain knowledge of discrete audio signals and systems better informs our decisions for an audio denoising system, so some background information on signals and systems as it pertains to this thesis is detailed below.

### 2.3.1 Signals

We deal exclusively with discrete-time audio signals in this thesis. A discrete-time audio signal  $x[n]$  is represented as a sequence of numbers (samples), where each integer-valued slot  $n$  in the sequence corresponds to a unit of time based on the sampling frequency  $f_s$ . This comes from sampling the continuous-time audio signal  $x_c(t)$ :

$$x[n] = x_c(nT) \quad (1)$$

where  $T = 1/f_s$ . For example, a 1-second speech signal sampled at 8kHz has 8000 samples. Furthermore, digital signals also have discrete valued sample amplitudes. For the purposes of this thesis, the bit depths of computers we use for analysis are high enough to allow for perfect reconstruction between continuous-time signals and digital signals.

We also assume signals collected have been properly sampled according to the Nyquist-Shannon sampling theorem, which states that a discrete-time signal must be sampled at at least twice the highest frequency present in the signal to prevent aliasing of different frequencies. For example, speech signals generally have information up to 8kHz, so many speech signals are sampled at 16kHz. Music is more complex in that signals often span up to about 20kHz, so CD quality recordings are often sampled at 44.1kHz or higher. For this thesis, we use recordings sampled at 44.1kHz or lower.

### 2.3.2 Convolution

The discrete-time convolution operation takes two sequences  $x[n]$  and  $h[n]$  and outputs a third sequence  $y[n] = x[n] * h[n]$ :

$$y[n] = \sum_{k=-\infty}^{\infty} x[k]h[n-k] \quad (2)$$

Convolution is commutative, so  $x[n] * h[n] = h[n] * x[n]$  holds true.

A linear, time-invariant (LTI) system is characterized by its impulse response  $h[n]$ , which allows us to determine samples  $y[n]$  when  $x[n]$  is subject to  $h[n]$ . For the purposes of this thesis, our underlying clean signal  $x[n]$  might be

subject to the conditions of an acoustic environment  $h[n]$  and crowd noise  $N[n]$ :

$$y[n] = h[n] * x[n] + N[n] \quad (3)$$

In this scenario, our system would attempt to recover  $h[n] * x[n]$  and possibly even  $x[n]$  if the acoustic environment were deemed “noisy enough” due to echo and reverberation.

One of our proposed systems also incorporates convolutional neural networks (CNN) which use convolutions between frames of samples instead of simple linear combinations (discussed later).

### 2.3.3 Frequency Transforms

In some of our proposed systems, we use a frequency transformed version of the input signal as a preprocessing step to the system input. While no new information is gained from transforming the input, networks often respond better to determining the value of the magnitude of varying frequencies at a time slice instead of the individual time samples.

The frequency transform we use in this thesis is the discrete-time Fourier transform (DTFT). A sequence of  $N$  discrete-time samples is transformed into another sequence of  $N$  samples where each index then corresponds to a frequency bin. The DTFT  $X[k]$  of a signal  $x[n]$  is given by the following:

$$X[k] = \sum_{n=0}^{N-1} x[n] W_N^{kn} \quad (4)$$

where the twiddle factor  $W_N$  is given by  $W_N = e^{-j(2\pi/N)}$ . Then the reconstruction of  $x[n]$  from  $X[k]$  is given by:

$$x[n] = \frac{1}{N} \sum_{k=0}^{N-1} X[k] W_N^{-kn} \quad (5)$$

In this thesis, we also exploit the main duality between the time and frequency domain using the convolution theorem, which states that convolution in time is equivalent to multiplication in frequency and vice versa:

$$\mathcal{F}\{h[n] * x[n]\} = H[k]X[k] \quad (6)$$

$$\mathcal{F}^{-1}\{H[k] * X[k]\} = h[n]x[n] \quad (7)$$

This allows us to effectively treat our network as a non-linear filter that can denoise small time/frequency slices of our noisy signal, which can then be pieced back together using overlap-add resynthesis. We detail this in the next section.

### 2.3.4 Windowing and Perfect Reconstruction

To window a signal is to multiply a window function  $w[n]$  by the frame, i.e.  $w[n]x[n]$  over the frame length  $N$ . Because we are training a network to denoise small segments of a larger audio signal, we window the signal segments. This accommodates the finite-length requirement of the DTFT and helps to prevent spectral leakage. [DSPBOOK]

Also, to be able to properly reconstruct our signal, we use a window function and corresponding overlapping frame percentage to accomplish perfect reconstruction. The corresponding overlapping frame percentage is set such that the window sums to a constant for all time. For example, a rectangular window  $w[n] = 1$  over an interval of length  $N$  has an overlap of 0% to sum to a constant 1 for all time. Another popular window is the Hanning window, defined over an interval  $N$  by the following:

$$w[n] = \frac{1}{2} \left( 1 - \cos \left( \frac{2\pi n}{N-1} \right) \right) \quad (8)$$

For the Hann window, the perfect reconstruction overlap is a frame length of  $N = 50\%$ .

### 2.3.5 Window Size and Frequency v. Time Resolution Tradeoff

We must consider window size as a hyperparameter to our system. In general, shorter windows give rise to better time resolution at the cost of frequency resolution. On the other hand, longer windows give rise to better frequency resolution at the cost of time resolution. To illustrate, consider FIGURE.

### 2.3.6 Noise and Signal-to-Noise Ratio

Since we are trying to denoise audio signals, we must discuss how we measure noise. One of the most common measures of degradation of signal quality from additive noise is signal-to-noise ratio (SNR), defined as the ratio of signal variance to noise variance. [DSP] For the signal  $y[n] = x[n] + N[n]$ , where  $x[n]$  is the signal of interest and  $N[n]$  is the additive noise, the SNR is defined as

$$SNR = \frac{\sigma_x^2}{\sigma_n^2} \quad (9)$$

where  $\sigma^2$  refers to the variance of the signal in question over some time interval. For the purposes of this thesis, we achieve desired a desired SNR for a simulation by scaling the noise to match the variance to the signal, then scaling the noise or the signal to achieve the desired SNR.

### 2.3.7 Magnitude and Phase Spectrum

### 3 Signal Model and Data

#### 3.1 Network Input and Output

To simulate an audio denoising scheme, we define the following inputs and outputs. We take a known clean signal  $x[n]$  which we subject to additive noise  $N[n]$  using a specified SNR, resulting in the following noisy signal  $y[n]$ :

$$y[n] = x[n] + N[n] \quad (10)$$

To achieve a particular average SNR per simulation, we take the average signal energy for each minibatch of size  $B$  to determine a multiplicative scale factor  $k$  on the noise signal  $N[n]$ . For example, for additive white Gaussian noise (AWGN), we sample from the zero-mean, unit variance normal distribution (“randn” in Python) and determine our scale factor  $k$  as  $\sigma$  using the specified SNR in decibels:

$$\sigma_n^2 = \frac{1}{SNR_{lin}} \frac{1}{BN} \sum_{b=0}^{B-1} \sum_{n=0}^{N-1} x_b^2[n] \quad (11)$$

where  $SNR_{lin}$  is given by

$$SNR_{lin} = 10^{\frac{SNR_{db}}{10}} \quad (12)$$

In supervised scenarios, we allow the network to train with access to the ground truth  $x[n]$ . On the other hand, in semi-supervised scenarios, we only allow the network to train with access to a “soft label” indicating if the signal is (1) noise-only or (2) noise and possibly signal. [DanStowell] However, in both supervised and semi-supervised scenarios, our neural network input is one of the following:



1. Frames of  $y[n]$
2. Frames of  $\|Y[k]\|$
3. Magnitude spectrogram frames of  $Y[k]$
4. Complex spectrogram frames of  $Y[k]$

We choose the frame length  $L$ , time-domain window  $w[n]$ , and frame overlap percentage  $p$  as hyperparameters. Generally, we use 1024-sample frames with a Hanning window with 50% overlap unless otherwise specified.

Since we want to evaluate the level of denoising in the time domain, we recombine the network outputs with the noisy phase components of the spectrum if necessary to obtain an estimate  $\hat{x}[n]$ . We then compare  $\hat{x}[n]$  to  $x[n]$ , in general using the mean squared error (MSE). For example, when our network outputs frames of  $\|\hat{X}[k]\|$ , we take the inverse Fast Fourier transform (IFFT) using the noisy phase  $\angle Y[k]$  and use overlap-add to recombine the frames. (Anything to add about phase denoising and failures here?)

### 3.2 Signal and Noise Choices

Our choice of signals include the following:

1. Sine waves with multiple frequencies and random amplitudes and phases
2. Clean speech signals
3. Studio music recordings
4. Live concert recordings

Similarly, our choice of noise signals include the following:

1. Additive white Gaussian noise (AWGN)
2. Restaurant noise

As mentioned above, we can use the average energy per minibatch to specify a given SNR for an experiment. We take several combinations of clean and noise signals and compare across multiple SNRs.

### 3.3 Other Network Parameters

Since our networks involve one or more neural network layers, we show some results compared to choices of nonlinearity, number of layers (depth), and number of nodes in each layer (width). Generally, we use an identity at the network output and either the rectified linear unit (ReLU), a modified ReLU (mReLU), leaky rectify, hyperbolic tangent (tanh), or an exponential linear unit (elu).

972	<b>4 De-noising Architectures</b>
973	
974	
975	<b>4.1 Classic Supervised Autoencoder</b>
976	
977	
978	<b>4.2 Paris Autoencoder</b>
979	
980	
981	<b>4.3 Partitioned Autoencoder</b>
982	
983	<b>4.3.1 Phase Reconstruction</b>
984	
985	
986	<b>4.4 Curro Autoencoder</b>
987	
988	
989	
990	
991	
992	
993	
994	
995	
996	
997	
998	
999	
1000	
1001	
1002	
1003	
1004	
1005	
1006	
1007	
1008	
1009	
1010	
1011	
1012	
1013	
1014	
1015	
1016	
1017	
1018	
1019	
1020	
1021	
1022	
1023	
1024	
1025	

## 5 Results

### 5.1 Classic Supervised Autoencoder

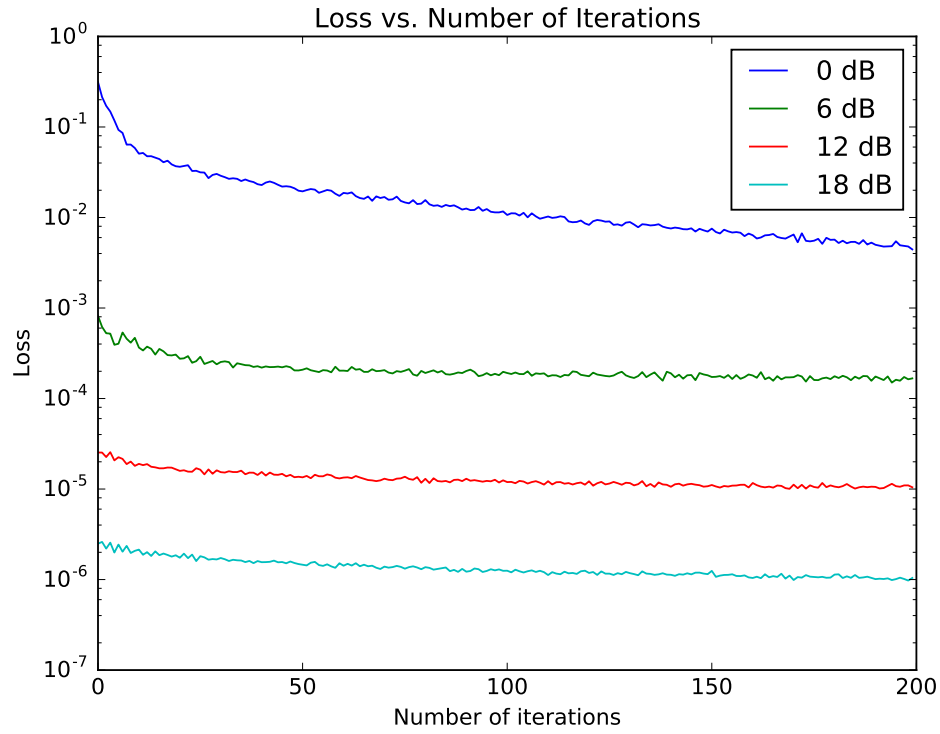


Figure 1

### 5.2 Paris Autoencoder

### 5.3 Partitioned Autoencoder

### 5.4 Curro Autoencoder

1080  
1081  
1082  
1083  
1084  
1085  
1086  
1087  
1088  
1089  
1090  
1091  
1092  
1093  
1094  
1095  
1096  
1097  
1098  
1099  
1100  
1101  
1102  
1103  
1104  
1105  
1106  
1107  
1108  
1109  
1110  
1111  
1112  
1113  
1114  
1115  
1116  
1117  
1118  
1119  
1120  
1121  
1122  
1123  
1124  
1125  
1126  
1127  
1128  
1129  
1130  
1131  
1132  
1133

## 6 Conclusions and Future Work

### 6.1 Conclusions

While more work is needed, deep partitioned neural network architectures using time and frequency data seem promising in long-term solutions for denoising speech and music signals.

### 6.2 Future Work

#### 6.2.1 Models

Make network deeper. Consider gradual partitioning instead of hard.

#### 6.2.2 Data

Get more data. Consider different noise levels and types of signals.

## References

- [1] A. Krizhevsky, I. Sutskever, and G. E. Hinton, “Imagenet classification with deep convolutional neural networks,” in *Advances in Neural Information Processing Systems 25*, F. Pereira, C. Burges, L. Bottou, and K. Weinberger, Eds. Curran Associates, Inc., 2012, pp. 1097–1105. [Online]. Available: <http://papers.nips.cc/paper/4824-imagenet-classification-with-deep-convolutional-neural-networks.pdf>
- [2] C. Szegedy, W. Liu, Y. Jia, P. Sermanet, S. Reed, D. Anguelov, D. Erhan, V. Vanhoucke, and A. Rabinovich, “Going deeper with convolutions,” *CoRR*, vol. abs/1409.4842, 2014. [Online]. Available: <http://arxiv.org/abs/1409.4842>
- [3] I. Sutskever, J. Martens, G. Dahl, and G. Hinton, “On the importance of initialization and momentum in deep learning,” in *Proceedings of the 30th International Conference on Machine Learning (ICML-13)*, 2013, pp. 1139–1147.
- [4] K. He, X. Zhang, S. Ren, and J. Sun, “Delving deep into rectifiers: Surpassing human-level performance on imagenet classification,” *CoRR*, vol. abs/1502.01852, 2015. [Online]. Available: <http://arxiv.org/abs/1502.01852>
- [5] G. E. Hinton, N. Srivastava, A. Krizhevsky, I. Sutskever, and R. Salakhutdinov, “Improving neural networks by preventing co-adaptation of feature detectors,” *CoRR*, vol. abs/1207.0580, 2012. [Online]. Available: <http://arxiv.org/abs/1207.0580>
- [6] D. R. Wilson and T. R. Martinez, “The general inefficiency of batch training for gradient descent learning,” *Neural Netw.*, vol. 16, no. 10, pp. 1429–1451, Dec. 2003. [Online]. Available: [http://dx.doi.org/10.1016/S0893-6080\(03\)00138-2](http://dx.doi.org/10.1016/S0893-6080(03)00138-2)
- [7] G. E. Dahl, T. N. Sainath, and G. E. Hinton, “Improving deep neural networks for lvcsr using rectified linear units and dropout,” in *Acoustics, Speech and Signal Processing (ICASSP), 2013 IEEE International Conference on*. IEEE, 2013, pp. 8609–8613.
- [8] M. D. Zeiler and R. Fergus, “Visualizing and understanding convolutional networks,” *CoRR*, vol. abs/1311.2901, 2013. [Online]. Available: <http://arxiv.org/abs/1311.2901>

- [9] S. Geman, E. Bienenstock, and R. Doursat, “Neural networks and the bias/variance dilemma,” *Neural computation*, vol. 4, no. 1, pp. 1–58, 1992.
- [10] X. Glorot and Y. Bengio, “Understanding the difficulty of training deep feedforward neural networks,” in *International conference on artificial intelligence and statistics*, 2010, pp. 249–256.
- [11] N. Srivastava, G. Hinton, A. Krizhevsky, I. Sutskever, and R. Salakhutdinov, “Dropout: A simple way to prevent neural networks from overfitting,” *Journal of Machine Learning Research*, vol. 15, pp. 1929–1958, 2014. [Online]. Available: <http://jmlr.org/papers/v15/srivastava14a.html>
- [12] J. Luo, “Frequently asked questions,” Hatfield Marine Science Center, 2014. [Online]. Available: <https://www.kaggle.com/c/datasciencebowl/data>
- [13] K. Fukushima, “Neocognitron: A self-organizing neural network model for a mechanism of pattern recognition unaffected by shift in position,” *Biological Cybernetics*, vol. 36, no. 4, pp. 193–202, 1980. [Online]. Available: <http://dx.doi.org/10.1007/BF00344251>
- [14] Y. LeCun, B. Boser, J. S. Denker, D. Henderson, R. E. Howard, W. Hubbard, and L. D. Jackel, “Backpropagation applied to handwritten zip code recognition,” *Neural computation*, vol. 1, no. 4, pp. 541–551, 1989.
- [15] X. Glorot, A. Bordes, and Y. Bengio, “Deep sparse rectifier networks,” in *Proceedings of the 14th International Conference on Artificial Intelligence and Statistics. JMLR W&CP Volume*, vol. 15, 2011, pp. 315–323.
- [16] Y. Nesterov *et al.*, “Gradient methods for minimizing composite objective function,” 2007.
- [17] A. Krogh and J. A. Hertz, “A simple weight decay can improve generalization,” in *ADVANCES IN NEURAL INFORMATION PROCESSING SYSTEMS 4*. Morgan Kaufmann, 1992, pp. 950–957.
- [18] R. Collobert, K. Kavukcuoglu, and C. Farabet, “Torch7: A matlab-like environment for machine learning,” in *BigLearn, NIPS Workshop*, no. EPFL-CONF-192376, 2011.
- [19] T. Salimans, I. J. Goodfellow, W. Zaremba, V. Cheung, A. Radford, and X. Chen, “Improved techniques for training gans,” *CoRR*, vol. abs/1606.03498, 2016. [Online]. Available: <http://arxiv.org/abs/1606.03498>

1242 [20] A. Radford, L. Metz, and S. Chintala, “Unsupervised repre-  
1243 sentation learning with deep convolutional generative adversarial  
1244 networks,” *CoRR*, vol. abs/1511.06434, 2015. [Online]. Available:  
1245 <http://arxiv.org/abs/1511.06434>  
1246  
1247  
1248 [21] E. L. Denton, S. Chintala, A. Szlam, and R. Fergus, “Deep  
1249 generative image models using a laplacian pyramid of adversarial  
1250 networks,” *CoRR*, vol. abs/1506.05751, 2015. [Online]. Available:  
1251 <http://arxiv.org/abs/1506.05751>  
1252  
1253  
1254 [22] Y. Li, K. Swersky, and R. S. Zemel, “Generative moment matching  
1255 networks,” *CoRR*, vol. abs/1502.02761, 2015. [Online]. Available:  
1256 <http://arxiv.org/abs/1502.02761>  
1257  
1258  
1259 [23] J. Johnson, A. Alahi, and F. Li, “Perceptual losses for real-time  
1260 style transfer and super-resolution,” *CoRR*, vol. abs/1603.08155, 2016.  
1261 [Online]. Available: <http://arxiv.org/abs/1603.08155>  
1262  
1263  
1264 [24] L. A. Gatys, A. S. Ecker, and M. Bethge, “A neural algorithm of  
1265 artistic style,” *CoRR*, vol. abs/1508.06576, 2015. [Online]. Available:  
1266 <http://arxiv.org/abs/1508.06576>  
1267  
1268  
1269 [25] A. Makhzani, J. Shlens, N. Jaitly, and I. J. Goodfellow, “Adversarial  
1270 autoencoders,” *CoRR*, vol. abs/1511.05644, 2015. [Online]. Available:  
1271 <http://arxiv.org/abs/1511.05644>  
1272  
1273  
1274 [26] L. Chen, G. Papandreou, I. Kokkinos, K. Murphy, and A. L. Yuille,  
1275 “Semantic image segmentation with deep convolutional nets and fully  
1276 connected crfs,” *CoRR*, vol. abs/1412.7062, 2014. [Online]. Available:  
1277 <http://arxiv.org/abs/1412.7062>  
1278  
1279  
1280 [27] F. Yu and V. Koltun, “Multi-scale context aggregation by dilated  
1281 convolutions,” *CoRR*, vol. abs/1511.07122, 2015. [Online]. Available:  
1282 <http://arxiv.org/abs/1511.07122>  
1283  
1284  
1285 [28] D. P. Kingma and J. Ba, “Adam: A method for stochastic  
1286 optimization,” *CoRR*, vol. abs/1412.6980, 2014. [Online]. Available:  
1287 <http://arxiv.org/abs/1412.6980>  
1288  
1289  
1290 [29] I. J. Goodfellow, J. Pouget-Abadie, M. Mirza, B. Xu, D. Warde-Farley,  
1291 S. Ozair, A. C. Courville, and Y. Bengio, “Generative adversarial  
1292 networks,” *CoRR*, vol. abs/1406.2661, 2014. [Online]. Available:  
1293 <http://arxiv.org/abs/1406.2661>  
1294  
1295



1296 [30] Y. A. LeCun, L. Bottou, G. B. Orr, and K.-R. Müller, “Efficient back-  
1297 prop,” in *Neural networks: Tricks of the trade*. Springer, 1998, pp. 9–48.  
1298  
1299  
1300 [31] A. G. Baydin, B. A. Pearlmutter, and A. A. Radul, “Automatic differ-  
1301 entiation in machine learning: a survey,” *CoRR*, vol. abs/1502.05767,  
1302 2015. [Online]. Available: <http://arxiv.org/abs/1502.05767>  
1303  
1304 [32] J. Bergstra, O. Breuleux, F. Bastien, P. Lamblin, R. Pascanu, G. Des-  
1305 jardins, J. Turian, D. Warde-Farley, and Y. Bengio, “Theano: A cpu and  
1306 gpu math compiler in python,” in *Proceedings of the 9th Python in Sci-*  
1307 *ence Conference*, S. van der Walt and J. Millman, Eds., 2010, pp. 3 –  
1308 10.  
1309  
1310  
1311 [33] M. Abadi, A. Agarwal, P. Barham, E. Brevdo, Z. Chen, C. Citro,  
1312 G. S. Corrado, A. Davis, J. Dean, M. Devin, S. Ghemawat, I. J.  
1313 Goodfellow, A. Harp, G. Irving, M. Isard, Y. Jia, R. Józefowicz,  
1314 L. Kaiser, M. Kudlur, J. Levenberg, D. Mané, R. Monga, S. Moore,  
1315 D. G. Murray, C. Olah, M. Schuster, J. Shlens, B. Steiner, I. Sutskever,  
1316 K. Talwar, P. A. Tucker, V. Vanhoucke, V. Vasudevan, F. B. Viégas,  
1317 O. Vinyals, P. Warden, M. Wattenberg, M. Wicke, Y. Yu, and  
1318 X. Zheng, “Tensorflow: Large-scale machine learning on heterogeneous  
1319 distributed systems,” *CoRR*, vol. abs/1603.04467, 2016. [Online].  
1320 Available: <http://arxiv.org/abs/1603.04467>  
1321  
1322  
1323 [34] G. Cybenko, “Approximation by superpositions of a sigmoidal function,”  
1324 *Mathematics of control, signals and systems*, vol. 2, no. 4, pp. 303–314,  
1325 1989.  
1326  
1327  
1328  
1329  
1330  
1331  
1332  
1333  
1334  
1335  
1336  
1337  
1338  
1339  
1340  
1341  
1342  
1343  
1344  
1345  
1346  
1347  
1348  
1349